



ARL-TR-7593 • FEB 2016



# Preparation of Copper (Cu)-Nickel (Ni) Thin Films for Bilayer Graphene Growth

by Andrew Chen, Eugene Zakar, and Robert Burke

Approved for public release; distribution is unlimited.

## **NOTICES**

### **Disclaimers**

The findings in this report are not to be construed as an official Department of the Army position unless so designated by other authorized documents.

Citation of manufacturer's or trade names does not constitute an official endorsement or approval of the use thereof.

Destroy this report when it is no longer needed. Do not return it to the originator.



# **Preparation of Copper (Cu)-Nickel (Ni) Alloy Thin Films for Bilayer Graphene Growth**

**by Andrew Chen and Eugene Zakar**  
*Sensors and Electron Devices Directorate, ARL*

**Robert Burke**  
*Contractor*

**REPORT DOCUMENTATION PAGE**

*Form Approved  
OMB No. 0704-0188*

Public reporting burden for this collection of information is estimated to average 1 hour per response, including the time for reviewing instructions, searching existing data sources, gathering and maintaining the data needed, and completing and reviewing the collection information. Send comments regarding this burden estimate or any other aspect of this collection of information, including suggestions for reducing the burden, to Department of Defense, Washington Headquarters Services, Directorate for Information Operations and Reports (0704-0188), 1215 Jefferson Davis Highway, Suite 1204, Arlington, VA 22202-4302. Respondents should be aware that notwithstanding any other provision of law, no person shall be subject to any penalty for failing to comply with a collection of information if it does not display a currently valid OMB control number.

**PLEASE DO NOT RETURN YOUR FORM TO THE ABOVE ADDRESS.**

<b>1. REPORT DATE (DD-MM-YYYY)</b> February 2016		<b>2. REPORT TYPE</b> Final		<b>3. DATES COVERED (From - To)</b> June–August 2015	
<b>4. TITLE AND SUBTITLE</b> Preparation of Copper (Cu)-Nickel (Ni) Alloy Thin Films for Bilayer Graphene Growth				<b>5a. CONTRACT NUMBER</b>	
				<b>5b. GRANT NUMBER</b>	
				<b>5c. PROGRAM ELEMENT NUMBER</b>	
<b>6. AUTHOR(S)</b> Andrew Chen, Eugene Zakar, and Robert Burke				<b>5d. PROJECT NUMBER</b>	
				<b>5e. TASK NUMBER</b>	
				<b>5f. WORK UNIT NUMBER</b>	
<b>7. PERFORMING ORGANIZATION NAME(S) AND ADDRESS(ES)</b> US Army Research Laboratory ATTN: RDRL-SER-L 2800 Powder Mill Road Adelphi, MD 20783-1138				<b>8. PERFORMING ORGANIZATION REPORT NUMBER</b>  ARL-TR-7593	
<b>9. SPONSORING/MONITORING AGENCY NAME(S) AND ADDRESS(ES)</b>				<b>10. SPONSOR/MONITOR'S ACRONYM(S)</b>	
				<b>11. SPONSOR/MONITOR'S REPORT NUMBER(S)</b>	
<b>12. DISTRIBUTION/AVAILABILITY STATEMENT</b> Approved for public release; distribution is unlimited.					
<b>13. SUPPLEMENTARY NOTES</b>					
<b>14. ABSTRACT</b> Co-sputtered copper (Cu)-nickel (Ni) alloys with layered thin-film ratios of 6:1, 4:1, and 3:1 were developed for use as a catalyst for the growth of graphene. A design of experiments was initiated with 3 tasks to complete: 1) metal preparation designed to achieve preferred (111) oriented films, 2) alloying of the layered films, and 3) the synthesis of AB-stacked quality bilayer graphene via low-pressure chemical vapor deposition (LPCVD). This report covers the analysis of the first 2 tasks by revealing the detailed morphological changes in the metal surfaces such as roughness, grain size, and crystal orientation due to the effects of annealing temperature, hydrogen (H <sub>2</sub> )/argon (Ar) gas ratio, and pressure. These variables are expected to have a major impact on the growth of graphene for different Cu-Ni thin-film concentrations.					
<b>15. SUBJECT TERMS</b> Growth, material, synthesis, deposition					
<b>16. SECURITY CLASSIFICATION OF:</b> Unclassified			<b>17. LIMITATION OF ABSTRACT</b>  UU	<b>18. NUMBER OF PAGES</b>  18	<b>19a. NAME OF RESPONSIBLE PERSON</b> Eugene Zakar
<b>a. REPORT</b> Unclassified	<b>b. ABSTRACT</b> Unclassified	<b>c. THIS PAGE</b> Unclassified			<b>19b. TELEPHONE NUMBER (Include area code)</b> 301-394-1628

## Contents

---

---

<b>List of Figures</b>	<b>iv</b>
<b>List of Tables</b>	<b>iv</b>
<b>1. Introduction</b>	<b>1</b>
<b>2. Experimental</b>	<b>2</b>
2.1 Metal Catalyst Preparation	2
2.2 Alloy and Grain Growth Conditions	3
<b>3. Results and Discussion</b>	<b>4</b>
3.1 Metal Catalyst Preparation and Characterization	4
3.2 Grain Growth Characterization	5
<b>4. Conclusion</b>	<b>9</b>
<b>5. Future Work</b>	<b>9</b>
<b>6. References and Notes</b>	<b>10</b>
<b>List of Symbols, Abbreviations, and Acronyms</b>	<b>11</b>
<b>Distribution List</b>	<b>12</b>

## List of Figures

---

---

Fig. 1	Cross-sectional drawing of the substrate after the metal deposition process.....	2
Fig. 2	Cross-sectional drawing of the substrate after the metal alloying step..	3
Fig. 3	XRD analysis of a) a commercial Alfa Aesar Cu foil #13382 and b) US Army Research Laboratory (ARL) thin film sputtered at a ratio of 6:1 Cu/Ni.....	4
Fig. 4	XRD analysis of 6:1 Cu-Ni thin film a) sputtered at 5 mT and 25 °C and b) sputtered at 15 mT and 400 °C .....	5
Fig. 5	AFM scan of 4:1 Cu-Ni thin film sputtered at 400 °C: a) as-deposited and b) post-annealed at 1000 °C for 30 min, 40% H <sub>2</sub> , 15 Torr.....	5
Fig. 6	AFM imaging of Cu:Ni alloyed films with ratios of a) 6:1 , b) 4:1, and c) 3:1 (all samples sputtered at 400 °C and annealed at 1000 °C for 30 min in 40% H <sub>2</sub> , and 15 Torr pressure) .....	6
Fig. 7	AFM imaging of Cu:Ni alloyed films with ratios of a) 6:1, b) 4:1, and c) 3:1 (all samples sputtered at 400 °C, annealed for 920 °C for 30 min in 40% H <sub>2</sub> , and 1.5 Torr pressure) .....	7
Fig. 8	AFM imaging of Cu:Ni alloyed films with ratios of a) 6:1, b) 4:1, and c) 3:1 (all samples annealed at 1025 °C for 30 min).....	8
Fig. 9	AFM imaging of Cu:Ni alloyed films with ratios of a) 6:1, b) 4:1, and c) 3:1 (all samples annealed at 800 °C for 17 h in 5% H <sub>2</sub> at atmosphere).....	8

## List of Tables

---

---

Table 1	Thin-film sputter deposition conditions.....	2
Table 2	Annealing parameters .....	3
Table 3	Measured step heights of Cu-Ni samples and calculated evaporation rates at 1025 °C.....	7

## 1. Introduction

---

Bilayer graphene has a tunable bandgap in a transverse electric field<sup>1-3</sup> making it a promising candidate for optoelectronic and nanoelectronic applications. Copper (Cu) is a favorable substrate for growth of monolayer graphene by chemical vapor deposition (CVD) process; however, the growth of a second layer would stop once the catalytic Cu surface is fully covered by 1 layer of graphene due to the self-limiting effect.<sup>4</sup> Recently, Cu-nickel (Ni) alloy foils have been used as a catalyst to achieve bilayer graphene growth. This was achieved by combining Cu, which has a small carbon (C) solubility (~0.0007% atom % at 1000 °C), with Ni, which has moderate C solubility (~1.3% atom % at 1000 °C), to form an alloy catalyst.<sup>5-6</sup> Researchers have achieved bilayer graphene growth with different Cu-Ni alloy concentrations ranging from 70% Cu to 90% Cu concentrations. In all the cases, the starting metal catalyst had mixed proportions of grain-oriented textures. The effect of different starting grain textures may have played a vital role in the out-diffusion rate of C that formed the bilayer graphene layers on extremely different Cu-Ni alloy concentrations. We would like to determine an optimum alloy composition on a preferred (111) grain-orientated texture material for direct comparison.

Prior studies of graphene growth have been performed on a limited selection of Cu-Ni compositions available in the form of cold rolled foils from various commercial foundries. Cu-Ni foils are typically available in concentrations of 90/10, 80/20, and 70/30 due to popular applications in marine and air conditioning fields. Commercial foils are of relatively low cost, but the plastic deformation from the rolling process typically results in non-ideal polycrystalline grain structures with variations of (100), (111), (110), and (311) textures that are not desirable for graphene growth. The initial orientation is expected to influence the evolution of grain size and stacking orientation of the graphene. Ideally, graphene crystallizes in a honeycomb structure, which is a hexagonal lattice. The symmetry of the (111) surface is hexagonal, whereas (100) and (110) are square and rectangular, respectively. From the symmetry perspective alone, it is expected that graphene grown on the (111) oriented surface should result in an over layer with the fewest rotational domains and produce the best electrical properties.

Commercial foils are also very rough with many ridges on the surface from the rolling process. Surface inconsistencies and impurities can act as nucleation sites for defects that will lead to variations in the growth and coverage of graphene layers. Foils require extensive pre-cleaning treatments prior to the graphene growth, which are an additional time-consuming burden and cost prohibitive for mass production.

Thin films of Cu-Ni, on the other hand, can be deposited in a vacuum chamber with higher purity and smoother surfaces, and achieve the preferred (111) grain-oriented texture without additional cleaning steps before graphene growth. We describe in this report the metal catalyst preparation steps and the alloying conditions needed to achieve bilayer graphene growth via low-pressure chemical vapor deposition (LPCVD).

## 2. Experimental

### 2.1 Metal Catalyst Preparation

The AJA ATC-2200 system was used to sputter deposit various ratios of Ni and Cu onto a 280-nm silicon dioxide (SiO<sub>2</sub>) coated silicon (Si) wafer. Since Ni is expected to be the primary contributor to bilayer graphene growth due to its high C solubility, varying amounts of Ni (50, 100, 150, and 200 nm) were sputter deposited as the base metal layer. A 600-nm layer of Cu was sputtered on top, as shown in Fig. 1.

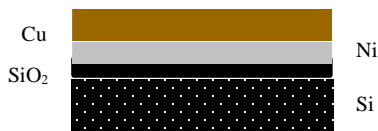


**Fig. 1** Cross-sectional drawing of the substrate after the metal deposition process

The combination of samples prepared, the Cu/Ni ratio, layer thickness, substrate sputter temperature, and sputter chamber pressure conditions are listed in Table 1. The Cu/Ni ratios in the range of 3:1 to 6:1 are expected to mix completely at 1000 °C and form alloys in the range of 70%Cu/30%Ni to 90%Cu/10%Ni, respectively. We show energy-dispersive x-ray spectroscopy (EDX) analysis later that confirms the bulk composition of the alloys.

**Table 1** Thin-film sputter deposition conditions

Sample No.	Cu/Ni Ratio	Layer Thickness (nm)	Temp (°C)	Pressure (mT)
1	6:1	(600 nmCu/100 nmNi)	25	5
2	6:1	(600 nmCu/100 nmNi)	25	15
3	6:1	(600 nmCu/100 nmNi)	400	5
4	6:1	(600 nmCu/100 nmNi)	400	15
5	4:1	(600 nmCu/150 nmNi)	25	5
6	4:1	(600 nmCu/150 nmNi)	25	15
7	4:1	(600 nmCu/150 nmNi)	400	5
8	4:1	(600 nmCu/150 nmNi)	400	15
9	3:1	(600 nmCu/200 nmNi)	25	5
10	3:1	(600 nmCu/200 nmNi)	25	15
11	3:1	(600 nmCu/200 nmNi)	400	5
12	3:1	(600 nmCu/200 nmNi)	400	15



## 2.2 Alloy and Grain Growth Conditions

The samples were loaded into a LPCVD furnace. The ramp-up rate was controlled at 100 °C/min until 600 °C, then 50 °C/min to 900 °C, and finally a 10 °C/min increase until the desired annealing temperature was reached without overshooting. Annealing was done at 1000 °C for a period of 30 min in a hydrogen (H<sub>2</sub>) + argon (Ar) gas mixture at 15 Torr pressure to reduce any existing metal oxides on the surface, enlarge the metal grain size, and form the Cu/Ni alloy, as shown in Fig. 2.

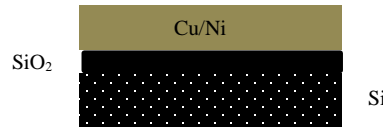


**Fig. 2** Cross-sectional drawing of the substrate after the metal alloying step

Several annealing parameters listed in Table 2 were investigated in order to determine the surface roughness, grain size, grain orientation, and film loss after the annealing and alloying process.

**Table 2** Annealing parameters

Temp (°C)	H <sub>2</sub> (vol. %)	Pressure (Torr)
800	5	0.025
920	20	15
1000	40	600
1025	100	atmosphere (ATM)

Characterization of the post-annealed Cu-Ni films was accomplished via atomic force microscopy (AFM) (Veeco Nanoman AFM), a surface profilometer (Tencor KLA-P15), x-ray diffraction (XRD) (Rigaku Cu K $\alpha$   $\lambda$ =1.540 Å, 40 kV, 44 mA), and optical microscopy.

The amount of film evaporation during the annealing process can be calculated by taking the difference between the as-deposited and post-annealed film thickness. A physical step height measurement of a film can be created by the following steps. A resist mask (AZ5214) is lithographically patterned over one half the surface of each sample after annealing. Transene brand APS-100 etchant is used to completely wet etch away the unmasked portion of the Cu-Ni alloy, and acetone is then applied to remove the photoresist mask to expose the Cu-Ni pattern. A KLA Tencor profilometer was used to scan across the patterned Cu-Ni alloy step height. Comparing the difference between the as-deposited and post-annealed step height measurement determines the film thickness loss.

### 3. Results and Discussion

#### 3.1 Metal Catalyst Preparation and Characterization

To match graphene's hexagonal-oriented carbon honeycomb structure, the optimal metal catalyst orientation should be (111). We generally use commercial Cu foils such as Alfa Aesar #13382; however, upon analysis with XRD, it was revealed that the Cu foil is predominantly (200) oriented (Fig. 3a) and not necessarily the best candidate for growing carbon lattices that match graphene domains.

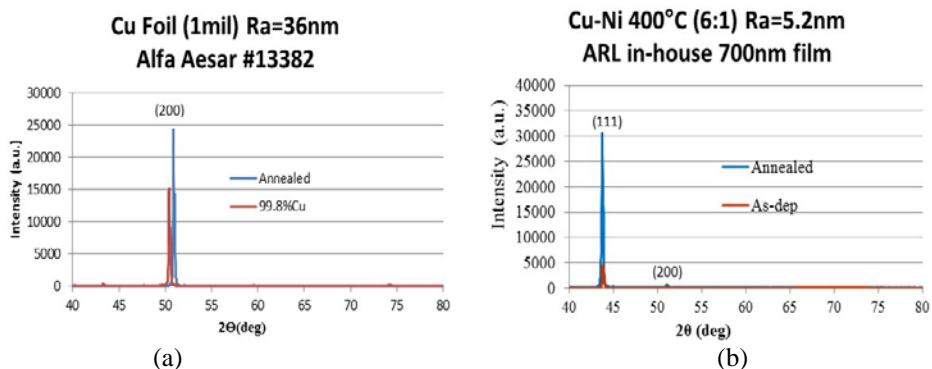


**Fig. 3** XRD analysis of a) a commercial Alfa Aesar Cu foil #13382 and b) US Army Research Laboratory (ARL) thin film sputtered at a ratio of 6:1 Cu/Ni

The ARL as-deposited sputtered Cu-Ni thin films, on the other hand, were found by XRD to be predominantly (111) oriented. After annealing, the crystalline quality of the film improved as evidenced by a narrower and sharper peak (Fig. 3b). The sputtering temperature and pressure were also found to have a pronounced effect on the grain orientations. While the films always remained (111) dominant, alloys prepared at a lower substrate temperatures (Fig. 4a) and higher pressures (Fig. 4b) produced additional minor facets such as (200), (220), and (311) in the films. Since only the (111) grain orientations are desired, the lower temperature sputtered samples and high pressure sputtering samples were not used in the remaining annealing studies.

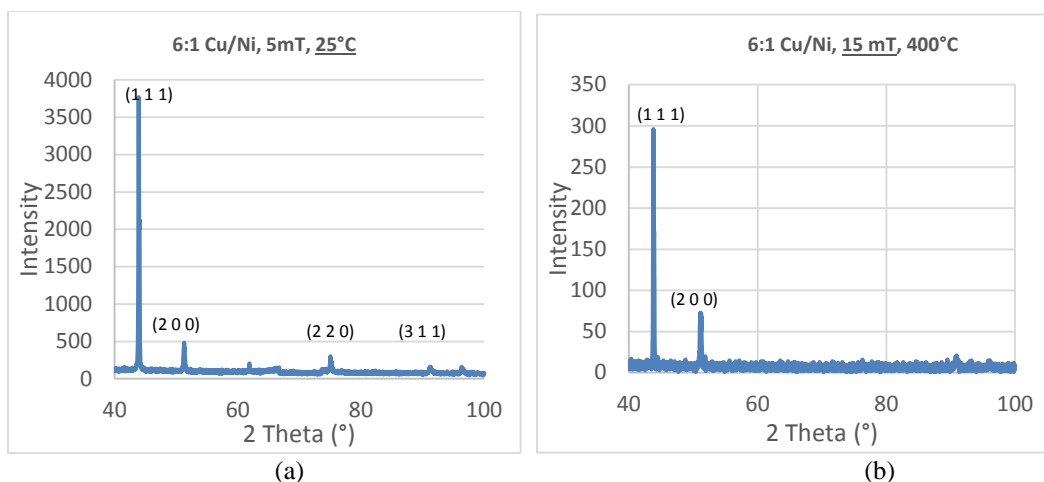


**Fig. 4** XRD analysis of 6:1 Cu-Ni thin film a) sputtered at 5 mT and 25 °C and b) sputtered at 15 mT and 400 °C

### 3.2 Grain Growth Characterization

The morphology of the as-deposited 4:1 Cu-Ni sample sputtered at a substrate temperature of 400 °C is shown in Fig. 5a and had an average roughness of 92.7 nm. Figure 5b shows the significant grain size enlargement after annealing at 1000 °C for 30 min and resulted in a much smoother average roughness of 66.1 nm.

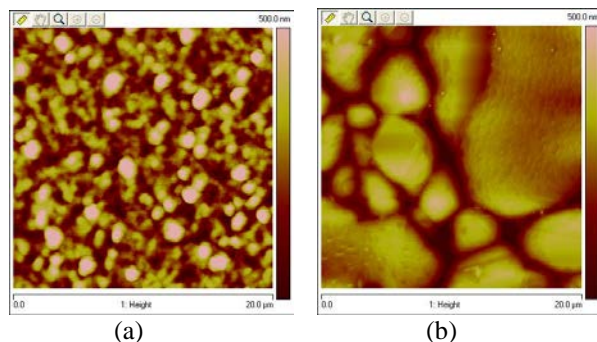


**Fig. 5** AFM scan of 4:1 Cu-Ni thin film sputtered at 400 °C: a) as-deposited and b) post-annealed at 1000 °C for 30 min, 40% H<sub>2</sub>, 15 Torr

After the annealing treatments, we analyzed the effect of Cu-Ni concentration on the grain size and roughness. As of the report date, the composition has not been identified due to service issues with our EDAX system. For practical purposes, in the remaining portion of the report, the samples continue to be identified by their film ratios. The films with ratios of 6:1, 4:1, and 3:1 in Fig. 6 have an average roughness of 86, 74, and 66 nm, respectively. The 6:1 Cu-Ni sample in Fig. 6a had the roughest surface features of the 3 samples with many particulates dispersed throughout the surface and numerous ridges/peaks above the grains themselves. These conditions are not ideal for graphene growth, because the particles and peaks

on the grain boundaries will serve as nucleation sites, which may promote multilayer graphene growth. As the Ni content in the Cu-Ni alloy is increased, there are noticeable improvements in both the roughness of the film and the grain size. The 4:1 Cu-Ni sample (Fig. 6b) shows a significant increase in the grain size with flattening of the grains with some of the larger grains averaging 10  $\mu\text{m}$  in diameter. There are almost no particles on the surface and considerably fewer ridges on the grains themselves. Increasing the Ni composition to 3:1 (Fig. 6c) further exemplifies this trend. The average grain size has increased and there is no evidence of particles or ridges in sight.

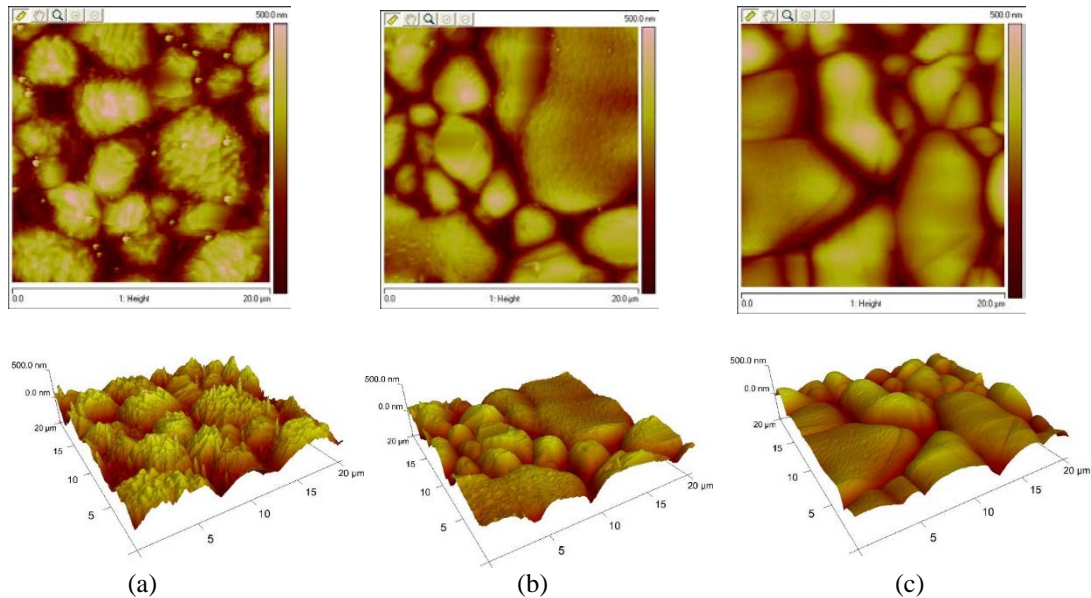


**Fig. 6** AFM imaging of Cu:Ni alloyed films with ratios of a) 6:1 , b) 4:1, and c) 3:1 (all samples sputtered at 400 °C and annealed at 1000 °C for 30 min in 40% H<sub>2</sub>, and 15 Torr pressure)

When the samples are annealed at a lower temperature (920 °C) and lower pressure (1.5 Torr) for 30 min, the final grains are comparatively smaller. There are many partially grown grains and incomplete grain boundaries in Fig. 7, which indicate that either a longer anneal time or a higher temperature is needed to see the grains grow to full maturity. There may be a slight increase in the evaporation rate of Cu due to the lower pressure and higher surface roughness. It also appears that the Cu:Ni with the lower film ratio of 3:1 has reduced particle density. Since grain growth responds well to temperature, a higher annealing temperature of 1025 °C is performed next to try and improve the grain size and possibly its flatness.

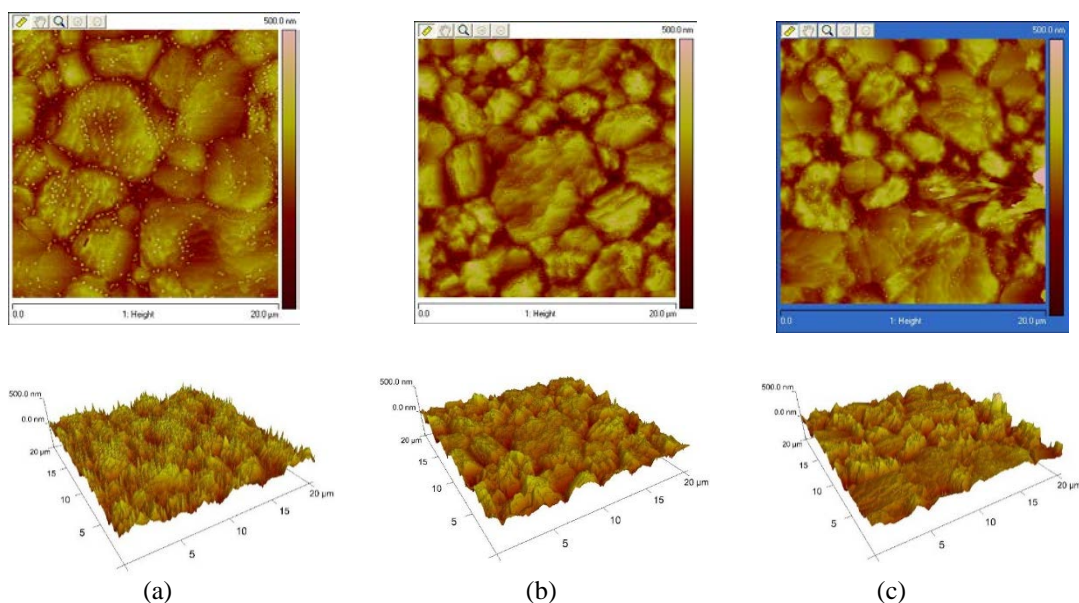


**Fig. 7** AFM imaging of Cu:Ni alloyed films with ratios of a) 6:1, b) 4:1, and c) 3:1 (all samples sputtered at 400 °C, annealed for 920 °C for 30 min in 40% H<sub>2</sub>, and 1.5 Torr pressure)

Annealing at a higher temperature of 1025 °C is, however, a concern because it nears the melting point of Cu, which is 1085 °C. After annealing, we determined the rate loss for each sample using the previously described step height measurement method. The evaporation rate was calculated by taking the difference in the step height before and after the annealing, then dividing by the annealing time. The results are listed in Table 3.

**Table 3** Measured step heights of Cu-Ni samples and calculated evaporation rates at 1025 °C

Ratio (Cu:Ni)	Sputter Temperature (°C)	Step Height As-deposited (nm)	Anneal Temperature (°C)	Step Height After Anneal (nm)	Evaporation Rate (nm/min)
6:1	400	700	1025	230	15.4
4:1	400	750	1025	240	16.9
3:1	400	800	1025	310	16.3

There does not appear to be any relationship between Cu-Ni ratio and the evaporation rate as all samples have an evaporation rate between the range of 15.4 to 16.9 nm/min, which represents a considerable loss of 61–68%, respectively, in film thickness. There also appears to be a significant increase in the surface roughness at the higher annealing temperature for the samples in Fig. 8.

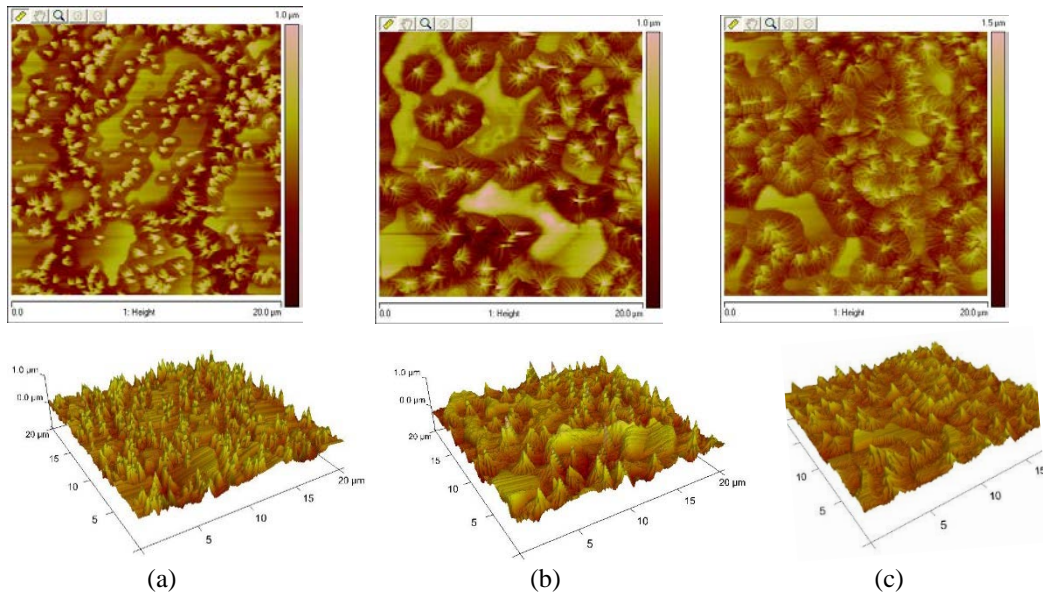


**Fig. 8** AFM imaging of Cu:Ni alloyed films with ratios of a) 6:1, b) 4:1, and c) 3:1 (all samples annealed at 1025 °C for 30 min)

When the annealing temperature was lowered to 800 °C and the pressure raised to atmosphere, the surface roughness diminished across all samples (Fig. 9) when compared to samples annealed at 1000 °C. The annealing was also extended to 17 h without much noticeable grain growth and surface roughness. It appears a combination of low temperature and high pressure has a favorable impact on the Cu-Ni alloy surface roughness.

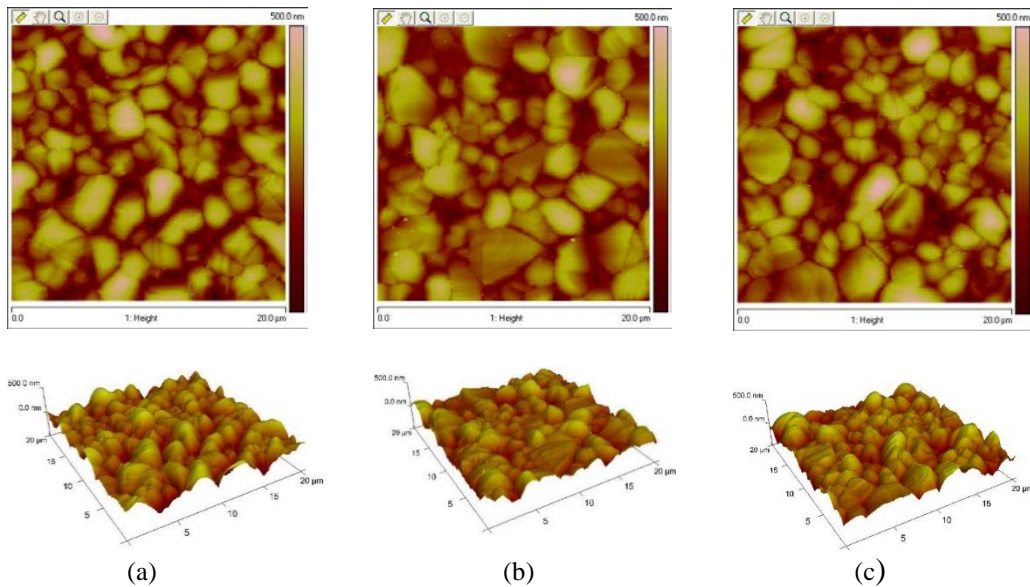


**Fig. 9** AFM imaging of Cu:Ni alloyed films with ratios of a) 6:1, b) 4:1, and c) 3:1 (all samples annealed at 800 °C for 17 h in 5% H<sub>2</sub> at atmosphere)

## 4. Conclusion

---

---

Cu-Ni alloyed thin films are very promising substrates as a catalyst for the growth of bilayer graphene. To obtain the preferred (111) metal surface orientation, sputter deposition should be performed at a low Ar pressure of 5 mT and a substrate temperature of 400 °C to produce low surface roughness. The Cu-Ni layers in the ratio range of 6:1, 4:1, and 3:1 produced predominantly (111) grain-oriented textures. The largest grain growth was observed when Cu-Ni samples were annealed at 1000 °C for 30 min in 40% H<sub>2</sub>. If samples were annealed at a relatively high temperature of 1025 °C for 30 min, a significant amount of film loss occurs due to evaporation. When annealed at 800 °C, there is insufficient grain growth, resulting in smaller grains. The roughness of the annealed samples appear to diminish with higher Ni concentration.

## 5. Future Work

---

---

More studies need to be conducted in terms of annealing before proceeding to the graphene growth step in order to fully understand the role of H<sub>2</sub> and pressure. This is particularly evident for samples with higher Cu concentrations that appear to be more vulnerable to surface roughening and potential film loss.

## 6. References and Notes

---

1. Gianluca F, Giuseppe I. Ultralow-voltage bilayer graphene tunnel FET. *IEEE Electron Device Lett.* 2009;30:1096–1098.
2. San JP, Prada E, Mc CE, Schomerus H. Pseudospin valve in bilayer graphene: towards graphene-based pseudospintronics. *Phys. Rev. Lett.* 2009;102:247204.
3. Kim KS, Zhao Y, Jang H, Lee SY, Kim JM, Kim KS, Ahn JH, Kim P, Choi JY, Hong BH. Large-scale pattern growth of graphene films for stretchable transparent electrodes. *Nature.* 2009;457:706–710
4. Li XS, Cai WW, An JH, Kim S, Nah J, Yang DX, Piner R, Velamakanni A, Jung I, Tutuc E, Banerjee SK, Colombo L, Ruoff RS. *Science.* 2009;324:1312–1314.
5. Fu L, Liu N, Gao T, Zhang Y, Liao L, Liu Z. Segregation growth of graphene on Cu–Ni alloy for precise layer control. *J. Phys. Chem. C.* 2011;11976-11982.
6. Wu Y, Chou H, Ji H, Wu Q, Chen S, Jiang W, Hao Y, Kang J, Ren Y, Piner RD, Ruoff RS. Growth mechanism and controlled synthesis of AB-stacked bilayer graphene on Cu-Ni alloy foils. *ACSNANO.* 2012.
7. Dunn WW, McLellan RB, Oates WA. The solubility of carbon in cobalt and nickel. *Trans. Metall. Soc. AIME.* 1968;242:2129.
8. Fang W, Hsu AL, Caudillo R, Song Y, Birdwell AG, Zakar E, Kalbac M, Dubey M, Palacios T, Dresselhaus MS, et al. Rapid identification of stacking orientation in isotopically labeled chemical-vapor grown bilayer graphene by Raman spectroscopy. *Nano Lett.* 2013;13:1541–1548.



## List of Symbols, Abbreviations, and Acronyms

---

AFM	atomic force microscopy
Ar	argon
ARL	US Army Research Laboratory
C	carbon
Cu	copper
CVD	chemical vapor deposition
EDX	energy-dispersive x-ray spectroscopy
H <sub>2</sub>	hydrogen
LPCVD	low pressure chemical vapor deposition
Ni	nickel
vol. %	volume percent
XRD	x-ray diffraction

1 DEFENSE TECHNICAL  
(PDF) INFORMATION CTR  
DTIC OCA

2 DIRECTOR  
(PDF) US ARMY RESEARCH LAB  
RDRL CIO LL  
IMAL HRA MAIL & RECORDS  
MGMT

1 GOVT PRINTG OFC  
(PDF) A MALHOTRA

17 DIRECTOR  
(PDF) US ARMY RESEARCH LAB  
RDRL SER E  
P AMIRTHARAJ  
R DEL ROSARIO  
F CROWNE  
E P SHAH  
T O'REGAN  
T IVANOV  
R FU  
G BIRDWELL  
RDRL SER L  
B PIEKARSKI  
M DUBEY  
E ZAKAR  
B NICHOLS  
M CHIN  
M ERVIN  
R BURKE  
A MAZZONI  
RDRL SEE  
M ROY